Co-Hydrothermal Carbonization of Sawdust and Sewage Sludge: Assessing the Potential of the Hydrochar as an Adsorbent and the Ecotoxicity of the Process Water

Matheus Cavali, Thuanne Braúlio Hennig, Nelson Libardi Junior, Boram Kim, Vincent Garnier, Hassen Benbelkacem, Rémy Bayard, Adenise Lorenci Woiciechowski, William Gerson Matias, Armando Borges de Castilhos Junior

Co-hydrothermal carbonization of sawdust and sewage sludge: assessing the potential of the hydrochar as an adsorbent and the ecotoxicity of the process water

Matheus Cavali[1*], Thuanne Braúlio Hennig[1], Nelson Libardi Junior[1], Boram Kim[2], Vincent Garnier[3], Hassen Benbelkacem[2], Rémy Bayard[2], Adenise Lorenci Woiciechowski[4], William Gerson Matias[1], Armando Borges de Castilhos Junior[1]

[1]Department of Sanitary and Environmental Engineering, Federal University of Santa Catarina, Florianópolis 88040-970, SC, Brazil; thuannebrauliohennig@gmail.com (T.B.H.); nelson.libardi@ufsc.br (N.L.J.); william.g.matias@ufsc.br (W.G.M.); armando.borges@ufsc.br (A.B.d.C.J.)
[2] DEEP Laboratory, EA 7429, National Institute of Applied Sciences of Lyon, 69621 Villeurbanne, France;; boram.kim@insa-lyon.fr (B.K.); hassen.benbelkacem@insa-lyon.fr (H.B.); remy.bayard@insa-lyon.fr (R.B.)
[3] MATEIS Laboratory, UMR 5510, National Institute of Applied Sciences of Lyon, 69621 Villeurbanne, France;; vincent.garnier@insa-lyon.fr
[4] Department of Bioprocess Engineering and Biotechnology, Federal University of Paraná, Curitiba 81531-908, PR, Brazil; adenise@ufpr.br
* Correspondence: cavali.matheus@gmail.com

Abstract: Hydrothermal carbonization (HTC) is a promising thermochemical process to convert residues into hydrochar. While conventional HTC utilizes one type of residue as raw material only, Co-HTC generally combines two. By mixing dry and wet wastes, Co-HTC can advantageously avoid water addition. Therefore, this work investigated the potential of hydrochar derived from the Co-HTC of sawdust and non-dewatered sewage sludge as a dye (methylene blue) adsorbent and evaluated the toxicity of the resulting Co-HTC process water (PW) on *Daphnia magna*. Three hydrochars were produced by Co-HTC at 180, 215, and 250 °C and named H-180, H-215, and H-250 respectively. For methylene blue adsorption, H-180 and H-215 had a better performance than H-250. Both H-180 and H-215 presented a maximum adsorption capacity of approximately 70 $mg \cdot g^{-1}$, which was superior compared with the adsorption of methylene blue by other hydrochars in the literature. Moreover, the removal percentage obtained with H-180 remained satisfactory even after five cycles. Regarding toxicological assays of PW, raising the Co-HTC temperature increased the variety of substances in the PW composition, resulting in higher toxicity to *D. magna*. The EC_{50} values of PW-180, PW-215, and PW-250 were 1.13%, 0.97% and 0.51%, respectively. However, it highlights the importance of searching for treatment and valorization of PW. Instead of viewing this by-product as an effluent to be treated and disposed of, it is imperative to assess the potential of PW for obtaining other higher added-value products.

Keywords: Hydrothermal carbonization; Adsorption; Methylene blue; Ecotoxicity; *Daphnia magna*; Waste valorization; Biochar

1. Introduction

The adverse effects of climate change have prompted discussions about the sustainability of current production systems. In this context, it is well-known that the transition from the current linear economic model to a circular one is necessary to achieve sustainable development. The circular economy also involves transforming waste into products, which can be understood as waste valorization approaches. Thus, research concerning waste valorization has been the subject of several studies about thermochemical processes, such as pyrolysis, gasification, and hydrothermal carbonization (HTC) [1–3].

Concerning HTC, its objective is to convert wastes into a solid, carbon-rich material named hydrochar. HTC has received great interest given the number of publications and established industries over the last decade [4]. In this process, waste is mixed with water at temperatures ranging from 180 to 350 °C under autogenous pressure conditions in sealed reactors [5]. The water between 100 and 374 °C becomes subcritical, acting not only as a solvent but also as a catalyst [6]. Advantageously, HTC uses water as the reaction medium, which is non-toxic, environmentally safe, and an economically cheap reagent [7]. Thus, HTC is convenient for wastes with high moisture content (e.g., sewage sludges), as it is carried out in an aqueous environment and does not require a pre-

drying stage [8]. Furthermore, the temperatures used in HTC are considerably lower than those used in pyrolysis and gasification processes.

When more than one waste is employed in HTC, the process is named Co-HTC, which is an interesting approach for combining wet and dry wastes [9]. Thus, Co-HTC is advantageous in circumventing some drawbacks of single-feedstock HTC. It can avoid dependence on only one feedstock, provide lower demands for water when wet wastes are used, and mitigate the inconvenience of an undesired waste characteristic, such as the high inorganic content [3]. For example, by combining inorganic-rich (e.g., sewage sludge) and inorganic-poor (e.g., sawdust) wastes, it is possible to improve the hydrochar characteristics compared with a hydrochar obtained only from the waste with a high content of inorganics [10–12]. The application of hydrochar depends on its characteristics. Hydrochar has the potential to be used, for example, for agriculture and crop improvement, catalyst support, carbon sequestration, electrochemical devices, and pollutant adsorption [13]. Regarding pollutant adsorption, hydrochar has been extensively proposed to remove heavy metals, nutrients, emerging contaminants, and dyes from aquatic environments [3].

Dye removal is a pertinent issue from wastewater from textile industries. Given the limited adsorption capacity of the fabrics, 85% of the dye mixture is discharged from the dyeing process. It makes textile industries the primary source of dye effluents in the environment because of the high usage of dyes in the coloring process [14]. If not properly managed, this could have adverse environmental consequences due to the dye toxicity [15]. It is therefore essential to implement effective dye removal methods to prevent the contamination of water sources by dye effluents. Among the proposed solutions, adsorption has been suggested as the best alternative because of its advantages, including high efficiency and short reaction times required [14,16]. Thus, sustainable and cost-effective adsorbents, such as hydrochar, can be a viable alternative for removing dyes from wastewater.

In addition to hydrochar, HTC or Co-HTC produces a liquid fraction named process water (PW) that generally presents acidic pH and high values of chemical oxygen demand (COD) [17]. According to the waste used in the HTC or Co-HTC, PW can present potentially toxic compounds, such as furfural, 5-hydroxymethylfurfural, phenol, cresol, catechol, resorcinol, and polycyclic aromatic hydrocarbons [18,19]. In the case of Co-HTC, PW can be more toxic due to the combination of different wastes. Despite that, studies evaluating the toxicity of the PW from Co-HTC processes are scarce in the literature [20,21]. It is important to understand the impact of HTC or Co-HTC PW in the environment to establish safe concentrations and design proper treatment and valorization processes.

Therefore, in light of the context mentioned above, the objectives of this study were (a) to evaluate the potential of hydrochar derived from the Co-HTC of sawdust and non-dewatered sewage sludge as a dye adsorbent and (b) to assess the ecotoxicity of the resulting PW.

2. Materials and Methods

2.1. Materials

The reagents employed in the experiments – $C_{16}H_{18}N_3ClS$ (methylene blue), sodium hydroxide (NaOH), hydrochloric acid (HCl), potassium dichromate ($K_2Cr_2O_7$), potassium hydroxide (KOH), and $C_4H_8O_2$ (ethyl acetate) – were of analytical grade.

Methylene blue was used as a model dye since it is a well-known dye employed by nearly all textile industries. This dye has found wide application in the dyeing of silk, wood, and cotton due to its absorbency and good fastness to materials. Methylene blue is a cationic and primary thiazine dye with a molecular weight of 319.85 $g \cdot mol^{-1}$, presenting a λ_{max} of 664 nm. It is highly water-soluble, forming a stable solution with water at room temperature [15,22–24].

2.2. Hydrochar production

The hydrochars from Co-HTC of sawdust and non-dewatered sewage sludge were produced according to the best conditions found in a previous study [12]. Co-HTC used a sawdust-to-sludge mass ratio of 10 for 2 to 3 h at 180, 215, and 250 °C. After filtration and drying, three hydrochars – H-180, H-215, and H-250, respectively – were obtained. The PW, named PW-180, PW-215, and PW-250, were properly stored for further utilization. Hydrochar yields and characteristics (e.g., volatile matter, ashes, and fixed carbon contents, O/C and H/C atomic ratios, Zeta potential, BET surface area), as well as the pH, COD, and electrical conductivity of PW, were described in previous studies [12,25]. Additionally, the point of zero charge (pH_{PZC}) was estimated by measuring Zeta potential (Malvern Zeta Sizer – Nano-ZSP) at pH 2, 4, 6, 8, 10, and 12 after mixing 20 mg of hydrochar with 20 mL of pH-adjusted deionized water at 20 °C for 24 h.

2.3. Adsorption of methylene blue

2.3.1. pH effect

To evaluate the pH influence in the methylene blue adsorption by H-180, H-215, and H-250, dye solutions of 100 mg·L^{-1} had their pH adjusted with NaOH and HCl (0.1 mol·L^{-1}) in the range from 2 to 10. The hydrochars and methylene blue solutions were mixed in Erlenmeyer flasks at a solid-to-liquid load of 3 g·L^{-1}. The mixture was stirred (100 rpm) for 24 h at 30 °C before separating the hydrochars from the methylene blue solution by vacuum filtration. The experiments were carried out in triplicate for each pH, in addition to blank tests (without hydrochar), and the mean, minimum, and maximum values were reported. The statistical analysis was conducted using the Origin® 2017 software.

2.3.2. Adsorption isotherms

At the best pH determined in the previous tests, the isotherms were performed for H-180 and H-215. The hydrochar and methylene blue solutions (25, 50, 100, 200, 300 400, 600, and 800 mg·L^{-1}) were mixed in Erlenmeyer flasks at a solid-to-liquid load of 3 g·L^{-1} The mixture was stirred (100 rpm) for 24 h at 30 °C before separating the hydrochars from the methylene blue solution by vacuum filtration. The experiments were carried out in triplicate for each isotherm point, in addition to blank tests (without hydrochar), and the mean, minimum, and maximum values were reported. The suitability of the Langmuir (Equation 1), Freundlich (Equation 2), and Sips (Equation 3) isotherm models for describing the data was evaluated [26]. The adjustment was performed in the software Origin® using the function *Nonlinear Curve Fit* and assessed according to R^2 and mean relative deviation (MRD) [27,28].

$$q_e = \frac{q_{max} \cdot K_L \cdot C_e}{1 + (K_L \cdot C_e)} \quad (1)$$

$$q_e = K_F \cdot C_e^{\frac{1}{n}} \quad (2)$$

$$q_e = \frac{q_{max} \cdot K_s \cdot {C_e}^n}{1 + (K_s \cdot {C_e}^n)} \quad (3)$$

In equations 1, 2, and 3, q_e is the adsorption capacity (mg·g^{-1}) at equilibrium, q_{max} is the maximum adsorption capacity (mg·g^{-1}) at equilibrium, K_L is the Langmuir constant, C_e is the concentration at the equilibrium (mg·L^{-1}), K_F is the Freundlich constant, n is an empirical constant related to the heterogeneity of the adsorbent surface, and K_S is the Sips constant. In Origin® 2017 software, the 95% confidence intervals for the q_{max} values of the hydrochars were calculated using the two-tailed Student's t-test to assess the variability of the estimates and to check whether the intervals overlapped.

2.3.3. Adsorption kinetics

Based on the previous tests, the adsorption kinetics were carried out for H-180. The hydrochar and methylene blue solutions (100 mg·L^{-1}) were mixed in Erlenmeyer flasks at a solid-to-liquid load of 3 g·L^{-1}. The mixture was stirred (100 rpm) at 30 °C, and sampled at 10, 15, 30, 45, 60, 90, 120, 180, 300, 480, 720, and 1440 min. After vacuum filtration, the concentration of the remaining methylene blue in the solution was determined. The experiments were carried out in triplicate for each point, in addition to blank tests (without hydrochar), and the mean, minimum, and maximum values were reported. The suitability of the non-linear pseudo-first-order (PFO – Equation 4), pseudo-second-order (PSO – Equation 5), and Elovich (Equation 6) models were tested [29,30]. The adjustment was performed in the software Origin® 2017 using the function *Nonlinear Curve Fit* and assessed according to R^2 and mean relative deviation (MRD) [27,28].

$$q_t = q_e \cdot (1 - e^{(-K_1 \cdot t)}) \quad (4)$$

$$q_t = \frac{K_2 \cdot {q_e}^2 \cdot t}{1 + (K_2 \cdot q_e \cdot t)} \quad (5)$$

$$q_t = \frac{1}{\beta} \cdot \ln(1 + \alpha \cdot \beta \cdot t) \quad (6)$$

In equations 4, 5, and 6, q_t and q_e are the adsorption capacity at time t and equilibrium, respectively ($mg \cdot g^{-1}$); t is the reaction time (min); K_1 (min^{-1}) and K_2 ($g \cdot mg^{-1} \cdot min^{-1}$) are the rate constants of PFO and PSO models, respectively; α is the initial adsorption rate ($mg \cdot g^{-1} \cdot min^{-1}$), and β is desorption constant ($g \cdot mg^{-1}$).

2.3.4. Adsorption thermodynamics

The adsorption thermodynamics was evaluated for H-180. The adsorption was carried out under different temperatures (30, 40, 50, and 60 °C). The hydrochar and methylene blue solutions (100 $mg \cdot L^{-1}$) were mixed in Erlenmeyer flasks at a solid-to-liquid load of 3 $g \cdot L^{-1}$ for 15 h. After vacuum filtration, the concentration of the remaining methylene blue in the solution was determined. The experiments were carried out in triplicate for each temperature, in addition to blank tests (without hydrochar). The changes in Gibbs free energy ($\Delta G°$, $J \cdot mol^{-1}$), enthalpy ($\Delta H°$, $J \cdot mol^{-1}$), and entropy ($\Delta S°$, $J \cdot mol^{-1} \cdot K^{-1}$) were obtained based on Equations 7, 8, 9, and 10 as described elsewhere [31].

$$\Delta G = -RT \cdot \ln(K_c) \quad (7)$$

$$K_c = \frac{C_0 - C_e}{C_e} \quad (8)$$

$$\Delta G = \Delta H - T\Delta S \quad (9)$$

$$\ln(K_c) = \frac{-\Delta H}{R} \cdot \frac{1}{T} + \frac{\Delta S}{R} \quad (10)$$

2.3.5. Hydrochar regeneration

The adsorbent regeneration was performed according to other studies to evaluate the hydrochar reusability [32–34]. A methylene blue solution of 100 $mg \cdot L^{-1}$ and pH 10 was mixed with hydrochar at a solid-to-liquid load of 3 $g \cdot L^{-1}$. The mixture was stirred (100 rpm) for 15 h at 30 °C before separating the hydrochar from the methylene blue solution by vacuum filtration. The desorption of methylene blue from hydrochar was carried out with ethanol. The dye-contaminated hydrochar was mixed with ethanol, stirred (100 rpm) for 5 h at 25 °C, vacuum filtered, washed with water, dried at 80 °C for 24 h, and reused for another adsorption cycle. The experiment was performed in triplicate for each cycle, and the mean, minimum, and maximum values were reported.

2.3.6. Methylene blue quantification

The remaining methylene blue concentration in the solution was determined with a UV-Vis spectrophotometer (Bel Photonics – UV-M51) at wavelength 664 nm based on a calibration curve (R^2 = 0.9960) previously prepared. The results were expressed as removal efficiency (%) and adsorption capacity ($mg_{dye} \cdot g_{hydrochar}^{-1}$) according to Equations 11 and 12, respectively. C_i and C_f are the initial and final dye concentration ($mg \cdot L^{-1}$), W is the hydrochar mass (g), and V is the volume of the dye solution (L).

$$RE = \frac{C_i - C_f}{C_i} \cdot 100 \quad (11)$$

$$q_e = \frac{(C_i - C_f) \cdot V}{W} \quad (12)$$

2.4. Process water (PW)

2.4.1. Ecotoxicity of PW

Acute toxicity tests were carried out on the microcrustacean *Daphnia magna* in accordance with OECD guideline 202 (2004). The *D. magna* culture was maintained at 20 ± 2 °C with a 16:8 light cycle. The medium was refreshed every two days, and daphnids were fed with microalgae *Desmodesmus subspicatus* three times weekly.

Based on preliminary tests, increased PW percentages of 1–1.4% for PW-180, 0.9–1.3% for PW-215, and 0.5–0.8% for PW-250 were tested, with no pH adjustment. A control with only dilution water was also included. Ten neonates (<24 hours old), verified for sensitivity via $K_2Cr_2O_7$ exposure, were placed in 25 mL of each test dilution. After 48 hours, immobility and concentrations that caused 50% effect (EC_{50}) values were assessed. The lower the EC_{50} value, the higher the inhibitory effect. Moreover, additional acute tests were conducted by exposing daphnids to the EC_{50} values of each PW, adjusting the pH of the exposure medium to 7 with NaOH, as recommended by OECD 202 (2004), to check the influence of pH on the toxicity of PWs.

Data analysis was conducted with GraphPad Prism® v6.0 and Statistica® v.13.5.0.17, using the Kolmogorov-Smirnov and Bartlett's tests for normality and homogeneity. EC_{50} values with 95% confidence intervals were calculated from logistic regression curves, and Dunnett's test ($p < 0.05$) compared treatment means to controls.

2.4.2. Characterization of PW

The analyses of COD and total nitrogen of PW-180, PW-215, and PW-250 followed the procedures 5220D and 4500N-C from the Standard Methods for the Examination of Water and Wastewater, respectively [35]. The effluents were also submitted to ionic liquid chromatography and gas chromatography coupled with mass spectrometry (GC-MS) analyses.

The ion chromatography analysis was performed to quantify the concentrations of acetate, chloride, nitrite, nitrate, sulphate, and phosphate. The analysis used an ion chromatography system (Thermo Scientific – DIONEX ICS-5000) with a DIONEX IonPac AS19 capillary column (2x250 mm). The eluent (EGC-KOH) was used in the following gradient mode: 10 mM KOH (0 to 10 min), 10 to 45 mM KOH (10 to 25 min), 45 mM KOH (25 to 30 min), and 10 mM KOH (30 to 35 min). The temperature was 30 °C, the flow rate was 0.250 mL·min^{-1}, and the injection volume was 1.5 mL under 2000 psi. The detection was obtained using a conductivity detector with a suppressor module.

For the GC-MS analysis, the samples were acidified to pH 2 using HCl, and 5 mL of ethyl acetate was added. After vigorous agitation for 2 min, it was allowed to stand for 1 h. Then, 1 mL was collected from the organic phase and injected into the GC–MS equipment. GC–MS analysis used a 5975C GC MSD gas chromatograph mass spectrometry (Agilent Technologies) equipped with an Agilent HP-5MS capillary column (30 m × 0.25 mm × 0.25 μm). Initially, the column temperature was held at 45 °C for 3 min, then programmed to 230 °C at a rate of 3 °C·min^{-1} with a hold time of 10 min, from 230 to 280 °C at a rate of 20 °C·min^{-1} and with a final hold time of 3 min. Helium was used as the carrier gas and the column head pressure was maintained at 83 kPa. The injector and detector temperatures were maintained at 250 and 300 °C respectively, and the injection volume was 1 μL in splitless mode. The interface temperature was held at 250 °C. Mass spectra were scanned from 30 m/z to 500 m/z at a rate of 1.5 scans·s^{-1}. Electron impact ionization energy was 70 eV [36].

3. Results and Discussion

3.1. Hydrochar production

The yields and characteristics of H-180, H-215, and H-250 were reported in a previous study, which addressed hydrochar production and characterization [12]. Table 1 summarizes the H-180,

H-215, and H-250 yield, volatile matter, ashes, fixed carbon, O/C and H/C atomic ratios, pH, zeta potential, and surface area.

Table 1. Yields and characteristics of hydrochar (H-180, H-215, and H-250) from Co-hydrothermal carbonization (Co-HTC) of sawdust and non-dewatered sewage sludge. Source: [12].

Hydrochar	Yield (%)	Volatile matter (%)*	Ashes (%)*	Fixed carbon (%)*	O/C	H/C	pH	BET surface area ($m^2 \cdot g^{-1}$)
H-180	87.3	78.5	10.4	11.1	0.5	1.3	5.4	14.8
H-215	72.7	74.4	8.0	17.6	0.4	1.2	5.2	9.6
H-250	64.1	59.3	18.4	22.3	0.2	0.9	5.8	22.7

**dry basis.*

The yield of hydrochar was observed to decrease in proportion to the increase in temperature, while the fixed carbon content was enhanced. The O/C and H/C atomic ratios exhibited a reduction when Co-HTC was conducted at 250 °C, indicating an improved carbonization at elevated temperatures. This condition also resulted in a hydrochar with a superior surface area compared to those obtained at 180 and 215 °C. All hydrochars had a natural pH of around 5.5 [12]. The Zeta potentials of H-180, H-215, and H-250 were -16, -17, and -21 mV, respectively [25].

The pH_{PZC} values of H-180, H-215, and H-250 were around 4. It means hydrochar is positively charged at a pH solution lower than 4 and negatively charged at a pH solution higher than 4. Therefore, at its natural pH, hydrochar presents a negatively charged surface, which could be useful for adsorbing cationic molecules, such as methylene blue.

3.2. Methylene blue adsorption

3.2.1. pH effect

Figure 1 presents the removal efficiency of methylene blue with H-180, H-215, and H-250. The results from each pH were submitted to ANOVA and Tukey tests at a 95% confidence level to ascertain whether there were statistically significant differences in the removal efficiencies of H-180, H-215, and H-250. The superior performance of H-180 and H-215 compared with H-250 is clearly noticeable for all pHs. At pH 2, H-215 outperformed H-180 and H-250 ($p_{value} < 0.05$). Conversely, at pH 4, the removal efficiency of H-180 and H-250 were equal ($p_{value} > 0.05$), whereas H-250 presented the lowest removal (9.4%) of all assays. For pH values of 6, 8, and 10, all hydrochars promoted different removal efficiencies ($p_{value} < 0.05$), but H-250 remained the least effective adsorbent, irrespective of pH. The removal efficiency was found to exceed 60% at pH values of 6, 8, and 10 for both H-180 and H-215. However, H-250 exhibited a significantly lower adsorption capacity, with an efficiency of approximately 20% across all hydrochars at those pH values. Interestingly, at pH 10, the methylene blue removal was slightly higher with H-180 than with H-215 ($p_{value} < 0.05$). It is a different trend in comparison with lower pH values, in which H-215, except for pH 4, presented superior removal efficiencies than H-180 ($p_{value} < 0.05$).

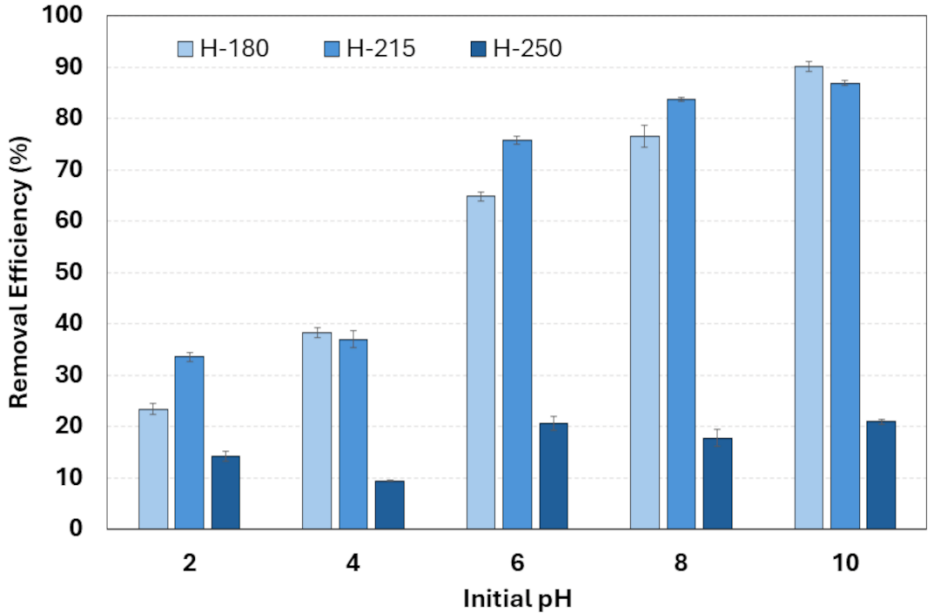

Figure 1. Influence of pH on methylene blue (100 mg·L^{-1}) adsorption (24 h at 30 °C and 100 rpm) by hydrochars (3 g·L^{-1}) from co-hydrothermal carbonization (Co-HTC) of sawdust and non-dewatered sewage sludge.

In aqueous solutions, methylene blue can exist in its cationic (MB^+) and as undissociated molecules (MB^0). MB^0 predominates at pH lower than 3.8, MB^0 (50%) and MB^+ (50%) coexisted equally at pH = 3.8, and MB^+ is the only species at pH > 6.0 [37]. Therefore, considering electrostatic interactions, one could explain the better adsorption performance of hydrochars at pH 6, 8, and 10 due to the hydrochars' pH_{PZC} and the pH-dependent methylene blue speciation. Even for H-250, it is possible to note a slight increase in the removal efficiency at pH 6, 8, and 10 compared with pH 2 and 4. Similarly, Khoshbouy and colleagues demonstrated that methylene blue removal was enhanced at basic pH due to the negative zeta potential of hydrochar, which was associated with elevated concentrations of OH^- ions and deprotonation of functional groups. This resulted in enhanced electrostatic attraction and hydrogen bond interactions between the hydrochar and dye [38].

The difference in removal efficiency of H-250 compared with H-180 and H-215 can be related to the surface functional groups of hydrochar. Hydrochars obtained from lignocellulosic materials can present oxygenated functional groups, such as phenolic, carboxylic, and lactonic, that can help with adsorption [39–41]. Under low temperatures, Co-HTC can preserve more oxygenated functional groups in the hydrochar surface [12], which could explain why H-180 and H-250 outperformed H-250. Li and colleagues demonstrated that methylene blue adsorption was more effective for hydrochar derived from Co-HTC of bamboo and polyvinyl chloride than for hydrochar produced from a single feedstock. This finding was attributed to the presence of a greater number of hydroxyl and carboxyl groups on the surface of the Co-HTC-derived hydrochar, which improved the adsorption of methylene blue [11]. Therefore, given their better performance than H-250, only H-180 and H-215 were considered for the following tests, which were carried out at pH 10.

3.2.2. Adsorption isotherms

Figures 2a and 2b show the isotherm of methylene blue adsorption by H-180 and H-215, respectively. The q_{max} for both hydrochars was around 70 mg·g^{-1}. Table 2 compares q_{max} for methylene blue of other hydrochars with that obtained in this study. The value obtained herein was similar to another hydrochar produced at 180 °C from citrus waste when the methylene blue adsorption was conducted at 4 °C, which q_{max} was 66 mg·g^{-1}; however, when the adsorption temperature was increased to 20 and 36 °C, q_{max} reduced to 51 and 31 mg·g^{-1}, respectively. In the same study, another hydrochar from winery waste also obtained at 180 °C presented q_{max} values between 29 and 37 mg·g^{-1} for adsorptions at 4, 20, and 36 °C, which are quite low compared with the results of this study. Additionally, it is worth noting that the BET surface area of citrus waste and winery waste hydrochars were 46 and 34 m²·g^{-1}, respectively, while the surface area of H-180 was 14.8 m²·g^{-1} [42]. Even with a lower surface area, the hydrochar from Co-HTC of sawdust and sewage sludge at 180 °C produced herein had a higher adsorption capacity for methylene blue. Another study used only sewage sludge for hydrochar production at 190, 220, and 250 °C and showed q_{max} of 71, 54, and 38 mg·g^{-1}, respectively, for methylene blue adsorption [43]. It is noteworthy that H-

180 exhibits a comparable q_{max} value to the hydrochar derived from the 190 °C treatment in the aforementioned study. Additionally, the H-215 displays a higher q_{max} value than the hydrochar obtained from the 220 °C treatment in the aforementioned study. Therefore, it demonstrates that combining wastes, such as lignocellulosic materials and sewage sludge, in a Co-HTC process can improve the adsorption capacity of hydrochar.

Despite the q_{max} obtained for H-180 and H-215, one can mention hydrochar activation to increase the adsorption capacity, as performed in some works [30,44–46]. However, it is important to consider that an activation step would result in increasing the costs of adsorbent production, in addition to the generation of effluents when using wet routes. Furthermore, some studies that performed hydrochar activation have demonstrated lower q_{max} values than those achieved for H-180 and H-215. For example, Lin and colleagues synthesized hydrochar from corn straw (HC), which was also N-dopped with urea (UHC), melamine (MHC), and NH_4Cl (AHC) to increase methylene blue adsorption. Nevertheless, the q_{max} values of all hydrochars obtained were lower than those of H-180 and H-215 (HC: around 10 $mg \cdot g^{-1}$; UHC: < 20 $mg \cdot g^{-1}$; MHC < 40 $mg \cdot g^{-1}$; AHC: < 60 $mg \cdot g^{-1}$) [47]. In another study, an oxide-hydrochar composite produced from pomegranate peels was activated with $ZnCl_2$, but the q_{max} value of the activated material was lowered to 50 $mg \cdot g^{-1}$ [48].

Table 2. Maximum adsorption capacity (q_{max}) of different hydrochars for methylene blue.

Raw material	Hydrochar activation	q_{max} ($mg \cdot g^{-1}$)	Reference
Sawdust and sewage sludge	No	70	This study
Citrus waste	No	31–66	[42]
Winery waste	No	2–37	
Sewage sludge	No	38–71	[43]
Corn straw	Yes	20–60	[47]
Pomegranate peels	Yes	50	[48]

The q_{max} of a carbon-derived adsorbent for methylene blue can vary significantly depending on the feedstock and production conditions utilized. This phenomenon has been extensively discussed in several review articles. For instance, Kasuma et al. reported a range of q_{max} values from 1.33 to 300 $mg \cdot g^{-1}$. Intriguingly, some activated carbons exhibited q_{max} values below 9 $mg \cdot g^{-1}$, notably lower than the values observed for H-180 and H-215 [22]. In another study, q_{max} values of carbon-based adsorbents – activated carbon, graphite porous carbon, and carbon nanotubes – ranged from 0.003 to 2936 $mg \cdot g^{-1}$, highlighting the variability in outcomes [49].

Figures 2a and 2b also present the adjustment of the experimental data regarding H-180 and H-215, respectively, to Langmuir, Freundlich, and Sips isotherm models, for which the parameter values are reported in Table 3. The Langmuir isotherm model assumes monolayer adsorption, whereby the adsorption process occurs exclusively on a homogeneous adsorbent surface with identical adsorption sites, forming a single layer of adsorbate molecules. Once a site is occupied, no further adsorption can occur at that site. Furthermore, the model assumes that the adsorption-desorption process is reversible. On the other hand, the Freundlich isotherm model assumes multilayer adsorption, which occurs on a heterogeneous surface with adsorption sites of varying energy levels. The molecules can adsorb onto each other after the initial layer has formed. Regarding the Sips isotherm model, it is a hybrid model obtained from the combination of both models aforementioned [50,51].

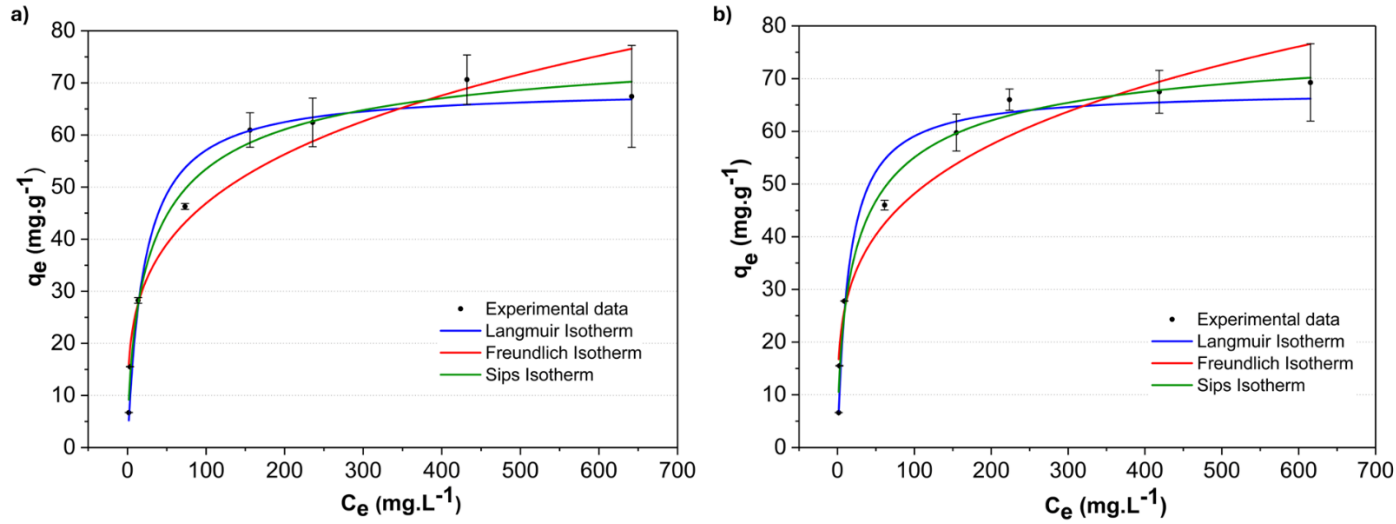

Figure 2. Isotherm models of methylene blue adsorption by H-180 (a) and H-215 (b) obtained at hydrochar load of 3 g·L^{-1} at pH 10, 30 °C, 100 rpm for 24 h.

Considering the R^2 and MRD values in Table 3, the Sips isotherm model is suggested for describing the methylene blue adsorption by both H-180 and H-215. This model indicated a q_{max} value of around 80 mg·g^{-1}. Additionally, no significant difference was noticed for both hydrochars regarding their adsorption performance since the 95% confidence intervals for q_{max} values of H-180 and H-215 overlapped. Thus, only H-180 was used in the following tests considering energy-saving purposes. It is preferable to conduct Co-HTC at 180 °C rather than at 215 °C.

Table 3. Values of parameters related to Langmuir, Freundlich, and Sips isotherm models.

Isotherm model	Parameter	H-180	H-215
Langmuir	q_{max} (mg·g^{-1})	69.01± 2.93 (56.40–81.61)*	67.78 ± 2.83 (55.60–79.96)*
	K_L	0.048 ± 0.012	0.068 ± 0.018
	R^2	0.9669	0.9636
	MRD (%)	11.56	9.89
Freundlich	K_F	13.92 ± 3.08	14.87 ± 3.09
	n	3.79 ± 0.57	3.92 ± 0.58
	R^2	0.9258	0.9289
	MRD (%)	25.54	27.68
Sips	q_{max} (mg·g^{-1})	80.35 ± 7.18 (49.45–111.25)*	79.96 ± 7.23 (48.85–111.07)*
	K_S	0.090 ± 0.020	0.112 ± 0.022
	n	0.672 ± 0.100	0.647 ± 0.099
	R^2	0.9852	0.9850
	MRD (%)	9.26	11.96

**95% confidence interval.*

3.2.3. Adsorption kinetics

Figure 3a presents the removal percentage of methylene blue with H-180 in the time. The adsorption increases rapidly in the first 3 h, reaching almost 60% of removal. From 13 h onwards, around 80% of methylene blue was removed and this removal percentage remained practically

constant until 24 h. According to other studies that also evaluate methylene blue adsorption by hydrochar, a significant number of adsorption sites were occupied by MB molecules as the adsorption time increased, resulting in a gradual slowing down of the subsequent mass transfer and adsorption process until equilibrium was reached [46,47,52]. In general, it is possible to identify three stages: 10-60 min, 90-480 min, and 720-1440 min. Akbari and colleagues suggest that, in the first stage, the presence of numerous vacant active sites on the surface of the adsorbent facilitates the interaction between methylene blue molecules and active sites, thereby achieving a high adsorption rate. In the second stage, the rate of adsorption declines due to a reduction in the number of available active sites and driving force, which is attributable to a decrease in the concentration of methylene blue. In the final stage, the reduction in the number of vacant active sites and dye concentration, coupled with the rise in electrostatic repulsion forces resulting from the adsorption of cationic molecules on the surface, might be the causes of the observed slow and steady adsorption rate, indicating that equilibrium was reached [53].

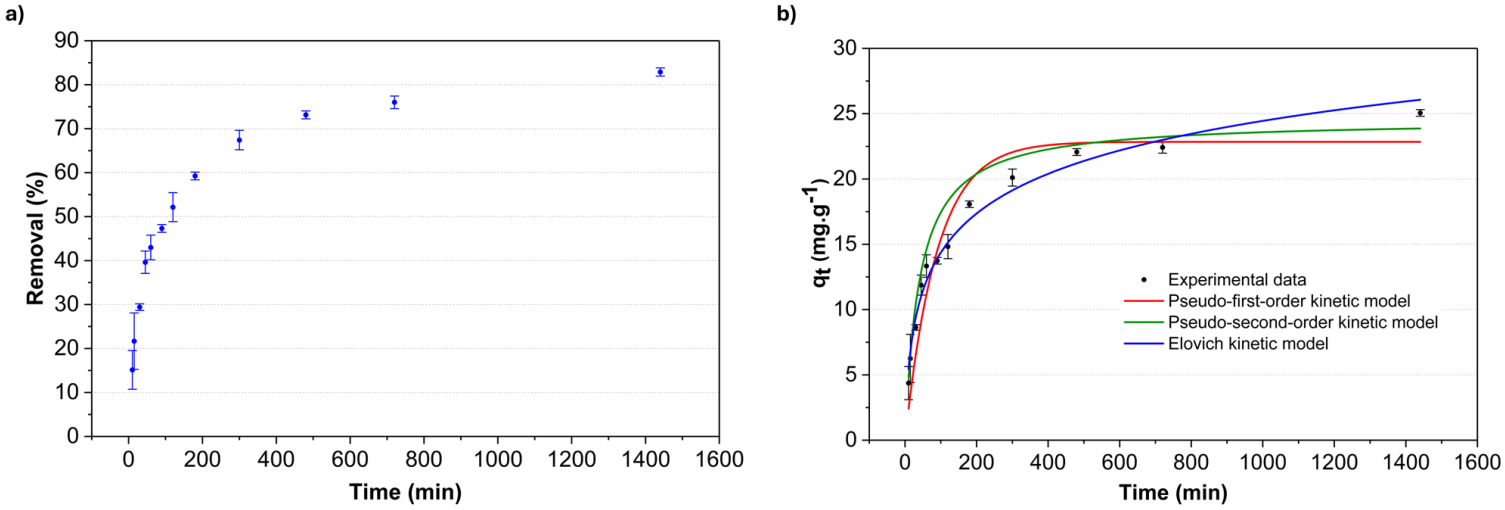

Figure 3. Removal percentage (a) and kinetics models (b) of methylene blue adsorption by hydrochar (H-180) obtained with an initial dye concentration of 100 mg·L^{-1} and a hydrochar load of 3 g·L^{-1} at pH 10, 30 °C, and 100 rpm.

In Figure 3b, kinetic models (PFO, PSO, and Elovich) were adjusted to the experimental data. As shown in Table 4, the Elovich kinetic model fits better than the others, considering the R^2 and MRD values. The suitability of the Elovich model compared with PFO and PSO models was also reported in another study of methylene blue adsorption by hydrochar [30]. The Elovich equation is suitable for describing chemisorption in systems with heterogeneous adsorbing surfaces [30,54–56], suggesting therefore this type of adsorption between H-180 and methylene blue.

Table 4. Values of parameters related to pseudo-first-order (PFO), pseudo-second-order (PSO), and Elovich kinetic models.

Kinetic Model	Parameter	H-180
Pseudo-First-Order	K_1	0.011 ± 0.001
	q_e (mg·g^{-1})	22.85 ± 0.85
	R^2	0.9124
	MRD (%)	5.57
Pseudo-Second-Order	K_2	0.001 ± 0.0002
	q_e (mg·g^{-1})	24.54 ± 1.11
	R^2	0.8909
	MRD (%)	7.09
Elovich	β	0.225 ± 0.012

α	1.08 ± 0.19
R^2	0.9779
MRD (%)	2.81

3.2.4. Adsorption thermodynamics

Table 5 presents the thermodynamics parameters of the methylene blue adsorption by H-180, obtained by linearizing Equation 7 (Figure 4). The value of Gibbs free energy change (ΔG) tends to become more negative as the temperature increases from 30 to 60 °C. This suggests that increasing the temperature favors the spontaneity of the process. Also, the positive value of enthalpy change (ΔH) indicates that the process is endothermic. In this instance, the positive value of entropy change (ΔS) is advantageous for the spontaneity of adsorption, as it makes ΔG negative by compensating for ΔH, thereby facilitating the occurrence of adsorption. This corroborates with previous studies using other hydrochars for adsorbing methylene blue [30,42].

Table 5. Thermodynamics parameters of the methylene blue adsorption by hydrochar (H-180) from co-hydrothermal carbonization (Co-HTC) of sawdust and non-dewatered sewage sludge.

ΔG (J·mol^{-1})	ΔS (J·mol^{-1}·K^{-1})	ΔH (J·mol^{-1})
-3845.12 (30 °C)	28.34	4746.13
-4128.52 (40 °C)		
-4411.92 (50 °C)		
-4695.32 (60 °C)		

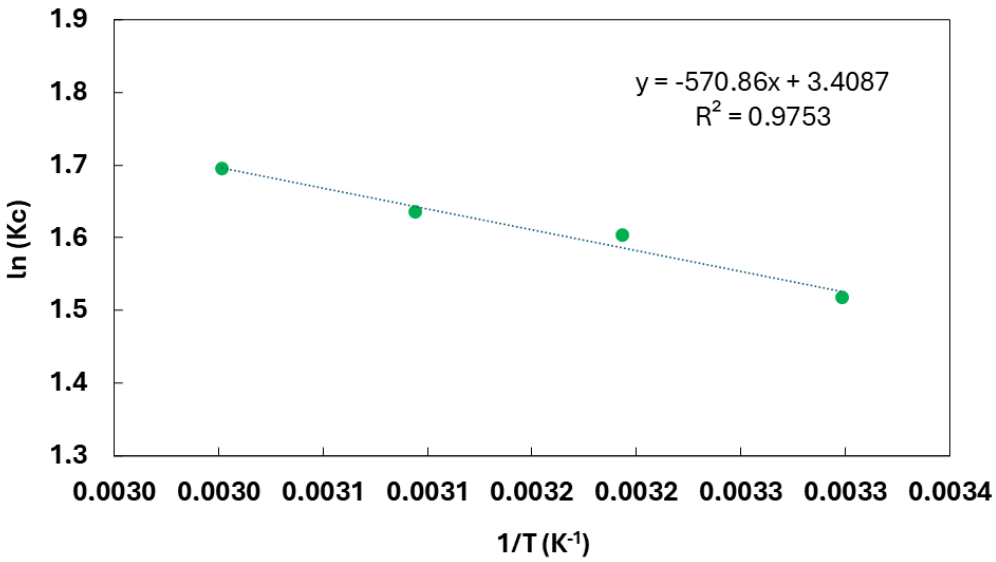

Figure 4. Linearization of Equation 7 to obtain the thermodynamic parameters of the methylene blue adsorption by hydrochar (H-180) from co-hydrothermal carbonization (Co-HTC) of sawdust and non-dewatered sewage sludge.

3.2.5. Hydrochar regeneration

Five cycles of methylene blue adsorption were performed to evaluate the reusability of H-180. Figure 5 presents the removal percentage of methylene blue for each cycle. It is worth noting that after five cycles the removal percentage remained around 80%; it decreased from 92.5% (first cycle) to 79.2% (fifth cycle). This represents a reduction of only 14.4% in relation to the first cycle. For comparison purposes, Akbari and colleagues reported a removal percentage reduction from

85% (first cycle) to 77% (fourth cycle) in methylene blue adsorption by hydrochar from liquorice root pulp. According to the authors, the changes to the adsorption sites on the adsorbent surface reduce the removal after each cycle. This occurs because some methylene blue molecules attach permanently to the surface, blocking the vacant pores and reducing dye adsorption efficiency [53].

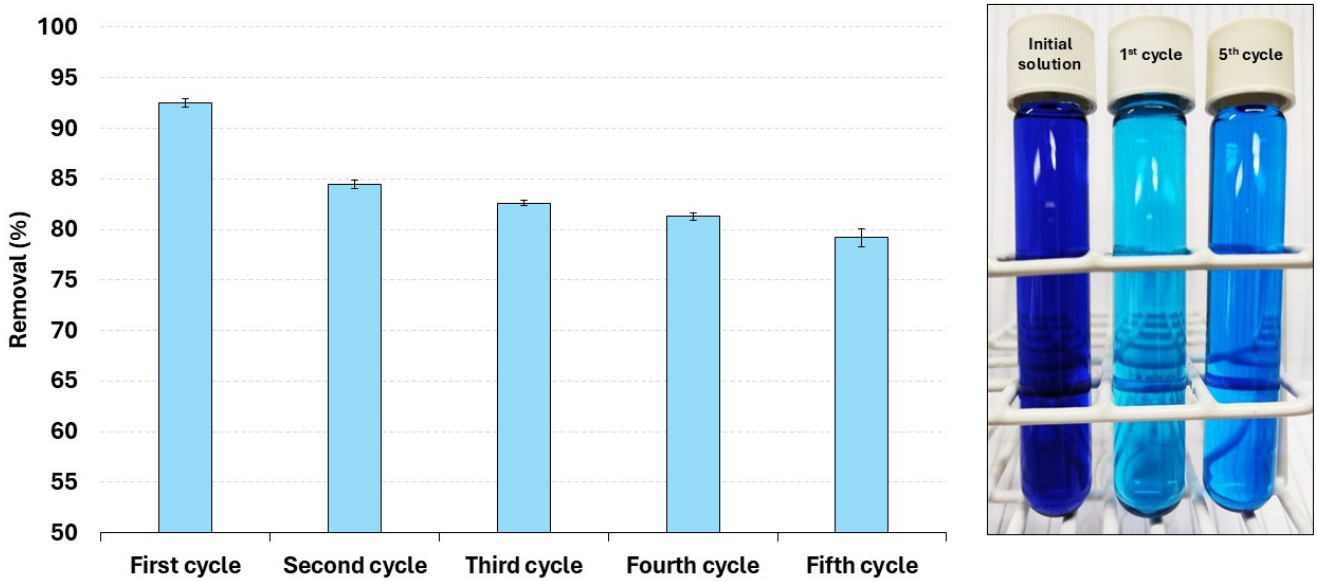

Figure 5. Removal percentage of methylene blue adsorption after five cycles by hydrochar (H-180) using an initial dye concentration of 100 mg·L^{-1} and a hydrochar load of 3 g·L^{-1} at pH 10, 30 °C, and 100 rpm for 16 h.

3.3. Process water (PW) – ecotoxicity and characterization

The acute toxicity test with PW-180, PW-215, and PW-250 was carried out on the microcrustacean *Daphnia magna* following OECD guideline 202 (2004) (Section 2.4.1). Exposure of *D. magna* to the PW-180, PW-215, and PW-250 showed high toxicity, with inhibitory effects observed after 48 h of exposure at the lowest percentage for all the PW tested. The effect was enhanced by increasing the PW concentration in the medium (Figure 6).

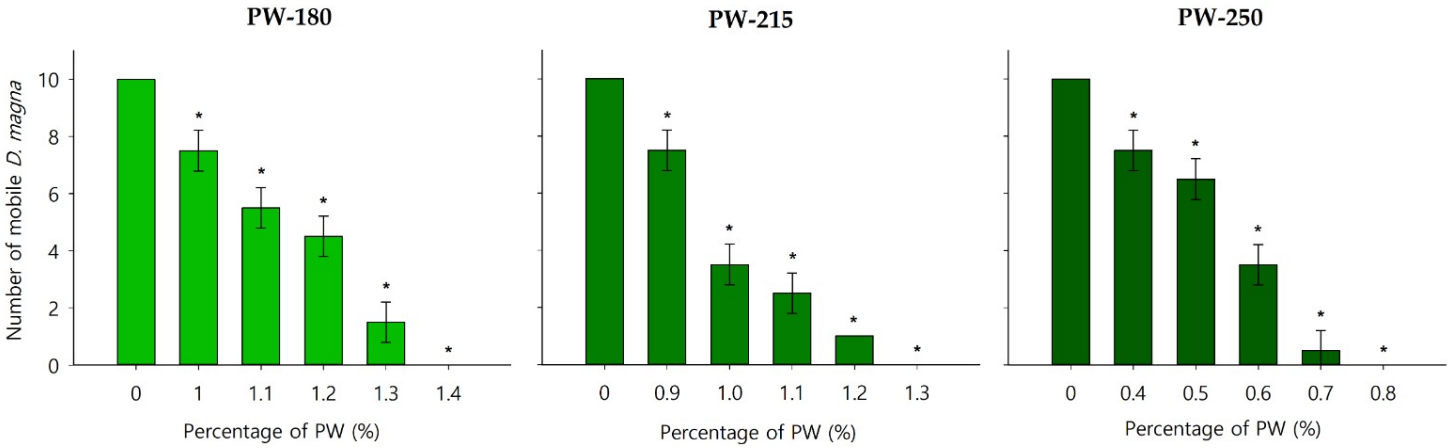

Figure 6. Average number of mobile *Daphnia magna* microcrustaceans (bars ± standard deviation, n = 6) after 48 hours of exposure to process water (PW) from co-hydrothermal carbonization (Co-HTC) of sawdust and non-dewatered sewage sludge at 180, 215, and 250 °C. Asterisks (*) represent a significant increase in the number of immobile microcrustaceans compared with the respective control (Dunnett's test, $p \leq 0.05$).

PW can be considered complex mixtures of dissolved organic compounds and nutrients (Tables 5 and 6). The COD of PW-180, PW-215, and PW-250 was 12.87 ± 0.55, 12.22 ± 0.35, 17.33 ± 0.75 g·L^{-1} [12]. Regarding total nitrogen, the values for PW-180, PW-215, PW-250 were 1.02 ± 0.09, 0.92 ± 0.06, and 1.00 ± 0.11 g·L^{-1}, respectively. Both parameters align with other PW reported in the literature, as presented in Table 6.

Table 6. Examples of chemical oxygen demand (COD) and total nitrogen values of process waters (PW) from hydrothermal carbonization (HTC) of different biomass wastes.

Waste	Hydrothermal carbonization condition*	Chemical oxygen demand (g·L^{-1})	Total nitrogen (g·L^{-1})	Reference
Agricultural residue digestate	T: 200; S/L: 1/5; t: 1	42.2	1.9	[57]
	T: 250; S/L: 1/5; t:1	46.3	2.2	
Municipal solid waste digestate	T:200; S/L: 1/5; t:1	18.1	2.4	
	T:250; S/L: 1/5; t:1	16.4	1.7	
Sewage sludge digestate	T:200; S/L: 1/5; t:1	38.9	4.5	
	T:250; S/L: 1/5; t:1	43.6	4.7	
Oat husk	T: 219.2; S/L: 1/12.5; t: 0.5	13.2	1.8	[58]
Water hyacinth	T: 150; S/L: 1/10; t: 1	19.0	-	[59]
	T:200; S/L: 1/10; t: 1	27.5	-	
	T:250; S/L: 1/10; t: 1	31.4	-	
Grape Marc	T:220; S/L: 1/10; t: 1	33.3	-	[60]
Grape Marc extracted		31.1	-	
Sewage sludge digestate	T: 160; S/L: 1/1; t: 0.5	12.6	-	[61]
	T: 220; S/L:1/1; t: 0.5	12.9	-	
	T: 250; S/L: 1/1; t: 0.5	12.2	-	

**T: temperature (°C); S/L: solid-to-liquid ratio; t: time (h).*

The presence and interaction of PW compounds in the exposure medium probably resulted in the toxic effects observed for *D. magna* [62,63]. Petroviˇc and colleagues have shown the high toxicity of PW from Co-HTC of vegetable oil industry waste and sewage sludge to *D. magna* (EC_{50} = 0.5%-2%) [64]. In another study, the PW from HTC of microalgae was toxic to *Allivibrio fischeri* (EC_{50} = 1.8%) [65]. For *Lemna minor*, the PW from sewage sludge was also harmful, causing complete decay at a 10% dilution [66]. In all the studies mentioned, the justification for the effects observed is consistent with our findings, which are also related to the complexity of PW composition (Tables 7 and 8).

Table 7. Content of acetate, chloride, nitrite, nitrate, sulphate, and phosphate in the process water (PW) from co-hydrothermal carbonization (Co-HTC) of sawdust and non-dewatered sewage sludge at three temperatures (180, 215, and 250 °C).

Ion	PW-180	PW-215	PW-250
Acetate ($mg \cdot L^{-1}$)	3333.67 ± 18.21	3600.67 ± 76.20	4584.00 ± 27.31
Chloride ($mg \cdot L^{-1}$)	118.94 ± 1.10	120.70 ± 1.44	124.70 ± 0.64
Nitrite ($mg \cdot L^{-1}$)	7.62 ± 0.00	1.99 ± 0.03	*nd*
Nitrate ($mg \cdot L^{-1}$)	13.80 ± 0.31	6.60 ± 0.14	*nd*
Sulfate ($mg \cdot L^{-1}$)	90.72 ± 0.39	74.87 ± 0.90	85.45 ± 14.32
Phosphate ($mg \cdot L^{-1}$)	441.93 ± 0.99	203.47 ± 0.53	194.32 ± 1.54

nd: not detected.

When comparing the toxicities of PWs from co-HTC at different temperatures, the EC_{50} values indicated the highest toxicity for PW-250 > PW-215 > PW-180, with values of 0.51% (0.48%–0.54%), 0.97% (0.95%–1.00%), and 1.13% (1.09%–1.17%), respectively. These results suggest that the increase in Co-HTC temperature elevated the toxicity on *D. magna*. The observed increase in toxicity aligns with the rise in compound generation due to the temperature increase (Table 8). A possible explanation for this behavior could be the high level of acetate present in the PWs (Table 7). As lignocellulosic biomass, sawdust is composed mainly of cellulose, hemicellulose, and lignin [67]. During hydrothermal treatments, such as Co-HTC, acetyl groups on hemicellulose chains are cleaved and form acetic acid in the solution. Depending on process conditions (e.g., temperature), cellulose, hemicellulose, and lignin can undergo partial or complete degradation. The more severe the hydrothermal treatment, the more degradation products are generated, as confirmed by PW compositions in Table 6. For instance, the degradation of cellulose and hemicellulose monomers forms hydroxymethylfurfural and furfural, while lignin degradation produces phenolic compounds [68–70]. These molecules are intermediates for hydrochar formation [3]. Therefore, the increase in Co-HTC temperature favors the decomposition of organic biomass and catalyzes the formation of various other chemical substances that may be toxic [71,72]. Thus, PW became progressively more heterogeneous and toxic as the temperature rose.

Table 8. Compounds identified by GC-MS in the process water (PW-180, PW-215, and PW-250) from co-hydrothermal carbonization (Co-HTC) of sawdust and non-dewatered sewage sludge.

Process water	Retention time (min.)	Peak area (%)	Compound	CAS Number
PW-180	3.722	12.00	Isobutyl acetate	000110-19-0
	5.188	87.99	Furfural	000098-01-1
	6.120	2.32	Furfural	000098-01-1
	26.810	1.33	Cyclohexasiloxane, dodecamethyl-	000540-97-6
PW-215	3.657	4.15	Isobutyl acetate	000110-19-0
	5.135	5.60	Furfural	000098-01-1
	7.574	0.93	2-Cyclopenten-1-one, 2-methyl-	001120-73-6
	7.806	1.05	Ethanone, 1-(2-furanyl)-	001192-62-7

	10.049	2.33	2-Furancarboxaldehyde, 5-methyl-	000620-02-0
	12.661	7.74	1,2-Cyclopentanedione, 3-methyl-	000765-70-8
	15.510	14.07	Phenol, 2-methoxy-	000090-05-1
	17.071	3.05	2-Cyclopenten-1-one, 3-ethyl-2-hydroxy-	021835-01-8
	24.371	3.54	(Z)-4-Methyl-5-(2-oxopropylidene)-5H-furan-2-one	026474-45-3
	27.564	7.93	Phenol, 2,6-dimethoxy-	000091-10-1
	29.885	3.02	Vanillin	000121-33-5
	35.049	5.98	Homovanillyl alcohol	002380-78-1
	3.716	1.50	Isobutyl acetate	000110-19-0
	5.028	0.42	Pyrazine, methyl-	000109-08-0
	5.223	1.21	2-Cyclopenten-1-one	000930-30-3
	7.580	4.67	2-Cyclopenten-1-one, 2-methyl-	001120-73-6
	10.144	1.26	2-Cyclopenten-1-one, 3-methyl-	002758-18-1
	10.981	1.27	Phenol	000108-95-2
	11.467	1.99	2-Cyclopenten-1-one, 2,3-dimethyl-	001121-05-7
	12.773	6.22	1,2-Cyclopentanedione, 3-methyl-	000765-70-8
	13.248	1.39	2-Cyclopenten-1-one, 2,3-dimethyl-	001121-05-7
	15.551	21.46	Phenol, 2-methoxy-	000090-05-1
	20.240	0.42	Furan, 2,5-dihydro-2,5-dimethyl-	059242-27-2
PW-250	20.560	0.80	Creosol	000093-51-6
	21.724	5.04	Catechol	000120-80-9
	23.890	1.86	1,2-Benzenediol, 3-methoxy-	000934-00-9
	24.478	3.57	Phenol, 4-ethyl-2-methoxy-	002785-89-9
	26.804	1.31	Cyclohexasiloxane, dodecamethyl-	000540-97-6
	27.712	8.91	Phenol, 2,6-dimethoxy-	000091-10-1
	30.223	1.10	4-Hydroxy-2-methoxybenaldehyde	018278-34-7
	33.434	0.55	5-Hepten-3-yn-2-ol, 6-methyl-5-(1-methylethyl)-	063922-41-8
	33.933	0.51	Cycloheptasiloxane, tetradecamethyl-	000107-50-6
	35.102	3.86	Homovanillyl alcohol	002380-78-1
	39.589	1.12	Homovanillic acid	000306-08-1
	39.725	2.30	Homovanillic acid	000306-08-1

Although no data were found in the literature regarding the toxicity of PW generated from Co-HTC of sawdust and sewage sludge, similar results were observed in a study exposing *D. magna* to dilutions of PW produced from Co-HTC of sewage sludge and whey at different temperatures. The study showed that the temperature increase affected the composition of PW; the toxicity of PW produced at 250 °C was approximately four times higher than that obtained at 200 °C for the same reaction time [21]. These findings reinforce that temperature significantly impacts both the composition and toxicity of PW.

When the daphnids were exposed to the previously obtained EC_{50} values with the pH of the exposure medium adjusted to neutral, there was no change in toxicity levels (Figure 7). This indicates that the toxicity effects observed for PW at different Co-HTC temperatures were not influenced by the acidic pH of the exposure medium (pH_{PW-180}=5.8; pH_{PW-215}=5.3; pH_{PW-250}=5.1), but probably by the specific composition of each PW and the interactions among their chemical constituents (Tables 7 and 8). However, while this conclusion appears evident, it should be interpreted with caution, as the toxicity of individual compounds and mixtures within each PW has not been tested.

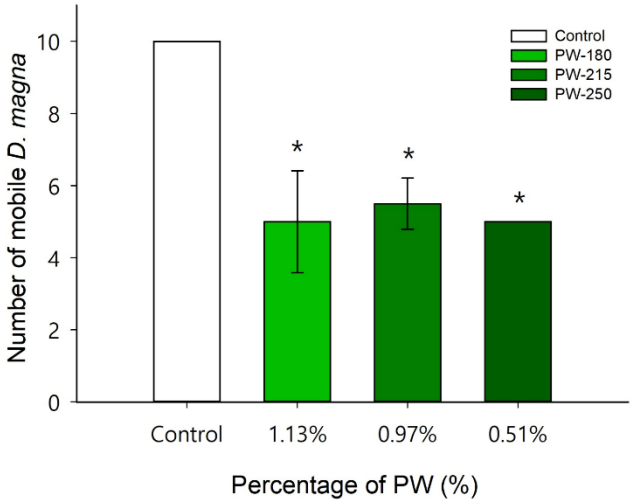

Figure 7. Average number of mobile *Daphnia magna* microcrustaceans (bars ± standard deviation, n = 6) after 48 hours of exposure to effect concentration values for 50% of exposed organisms (EC_{50}) previously obtained for process water (PW) from the co-hydrothermal carbonization (Co-HTC) sawdust and non-dewatered sewage sludge at 180, 215 and 250 °C with pH adjustment of the exposure medium with NaOH (pH = 7). The asterisks (*) represent a significant increase in the number of immobile microcrustaceans compared with the control test (Dunnett's test, $p \leq 0.05$).

These results underscore the necessity of identifying alternative methods for treating and, most crucially, valorization of PW to reduce its potential environmental impacts. Despite its toxicity, the PW from the Co-CHT of sawdust and sewage sludge contains molecules with commercial potential (e.g., furfural). Instead of viewing this by-product as an effluent to be treated and disposed of correctly in the environment, it is imperative to assess the potential of PW to obtain marketable products. For example, furfural, levulinic acid, vanillin, and catechol are considered platform chemicals, which are molecules that can serve as a substrate to produce a range of other higher value-added products [73–76].

4. Conclusion

This work assessed three hydrochars (H-180, H-215, and H-250) from Co-HTC of sawdust and non-dewatered sewage sludge as potential methylene blue adsorbents, and it also evaluated the ecotoxicological effects of the resulting PW. H-180 and H-215 had better adsorption performance than H-250. H-180 and H-215 presented a q_{max} value of around 70 $mg \cdot g^{-1}$, which was superior compared with the adsorption of methylene blue by other hydrochars in the literature. The Sips isotherm model was better than Langmuir and Freundlich models for describing the adsorption with H-180 and H-215. The Sips model indicated a q_{max} value of around 80 $mg \cdot g^{-1}$. It is noteworthy that H-180 and H-215 were not subjected to modification by physical or chemical activation, which could enhance their adsorption capacity. However, an activation step would also raise the production cost of the adsorbent. Compared with PFO and PSO models, the Elovich model presented a superior fit for describing the kinetics of methylene blue adsorption by H-180. Regarding the toxicological effects of the resulting PW on *Daphnia magna*, the high toxicity, especially at higher Co-HTC temperatures, underscores the need for careful management and further study to assess their environmental impact and potential valorization approaches.

Author Contributions: Conceptualization, M.C.; methodology, M.C., T.B.H., N.L.J., and B.K.; formal analysis, M.C., T.B.H., N.L.J., B.K., and V.G; investigation, M.C., T.B.H, N.L.J., B.K., and V.G; resources, N.L.J., B.K., V.G., H.B., R.B., A.L.W., W.G.M., and A.B.C.J.; data curation, M.C., T.B.H., N.L.J., and B.K.; writing – original draft preparation, M.C., T.B.H.; writing – review and editing, M.C., T.B.H., N.L.J., B.K., V.G., H.B., R.B., A.L.W., W.G.M., and A.B.C.J.; visualization, M.C. and T.B.H.; supervision, N.L.J., B.K., H.B., R.B., A.L.W., W.G.M., and A.B.C.J.; project administration, A.B.C.J.; funding acquisition, R.B., W.G.M., A.L.W., A.B.C.J. All authors have read and agreed to the published version of the manuscript.

Funding: Brazilian foundation Coordenação de Aperfeiçoamento de Pessoal de Nível Superior (CAPES) – Finance Code 001.

Institutional Review Board Statement: Not applicable.

Data Availability Statement: The original contributions presented in this study are included in the article. Further inquiries can be directed to the corresponding author.

Acknowledgments: The authors thank the Brazilian foundation Coordenação de Aperfeiçoamento de Pessoal de Nível Superior (CAPES), the laboratory of the graduate program in Bioprocess Engineering and Biotechnology of the Federal University of Paraná, and the DEEP (Déchets Eaux Environnement Pollutions) Laboratory of the Lyon National Institute of Applied Sciences (INSA Lyon) for the supervision and the analyses carried out. This work was performed within the framework of the EUR H2O'Lyon (ANR-17-EURE-0018) of Université de Lyon (UdL), within the program "Investissements d'Avenir" operated by the French National Research Agency (ANR).

Conflicts of Interest: The authors declare no conflict of interest.

References

1. Yu, C.; Chen, R.; Li, J.J.; Li, J.J.; Drahansky, M.; Paridah, M. t; Moradbak, A.; Mohamed, A.Z.; Owolabi, FolaLi, H. abdulwahab taiwo; Asniza, M.; et al. Pyrolysis: A Sustainable Way to Generate Energy from Waste. In *Intech*; 2012; p. 13.
2. You, S.; Sik, Y.; Chen, S.S.; Tsang, D.C.W.; Kwon, E.E.; Lee, J.; Wang, C. A Critical Review on Sustainable Biochar System through Gasification : Energy and Environmental Applications. *Bioresour Technol* **2017**, *246*, 242–253, doi:10.1016/j.biortech.2017.06.177.
3. Cavali, M.; Libardi Junior, N.; de Sena, J.D.; Woiciechowski, A.L.; Soccol, C.R.; Belli Filho, P.; Bayard, R.; Benbelkacem, H.; de Castilhos Junior, A.B. A Review on Hydrothermal Carbonization of Potential Biomass Wastes, Characterization and Environmental Applications of Hydrochar, and Biorefinery Perspectives of the Process. *Science of the Total Environment* 2023, *857*.
4. Prochnow, F.D.; Cavali, M.; Dresch, A.P.; Belli, I.M.; Libardi, N.; de Castilhos, A.B. Biochar: From Laboratory to Industry Scale—An Overview of Scientific and Industrial Advances, Opportunities in the Brazilian Context, and Contributions to Sustainable Development. *Processes* **2024**, *12*, 1006, doi:10.3390/pr12051006.
5. Parshetti, G.K.; Chowdhury, S.; Balasubramanian, R. Hydrothermal Conversion of Urban Food Waste to Chars for Removal of Textile Dyes from Contaminated Waters. *Bioresour Technol* **2014**, *161*, 310–319.
6. Zhao, K.; Li, Y.; Zhou, Y.; Guo, W.; Jiang, H.; Xu, Q. Characterization of Hydrothermal Carbonization Products (Hydrochars and Spent Liquor) and Their Biomethane Production Performance. *Bioresour Technol* **2018**, *267*, 9–16, doi:10.1016/j.biortech.2018.07.006.
7. Langone, M.; Basso, D. Process Waters from Hydrothermal Carbonization of Sludge: Characteristics and Possible Valorization Pathways. *Int J Environ Res Public Health* **2020**, *17*, 1–31, doi:10.3390/ijerph17186618.
8. Kambo, H.S.; Dutta, A. A Comparative Review of Biochar and Hydrochar in Terms of Production, Physico-Chemical Properties and Applications. *Renewable and Sustainable Energy Reviews* **2015**, *45*, 359–378, doi:10.1016/j.rser.2015.01.050.
9. Wang, Q.; Wu, S.; Cui, D.; Zhou, H.; Wu, D.; Pan, S.; Xu, F.; Wang, Z. Co-Hydrothermal Carbonization of Organic Solid Wastes to Hydrochar as Potential Fuel: A Review. *Science of the Total Environment* 2022, *850*.
10. Shan, G.; Li, W.; Bao, S.; Li, Y.; Tan, W. Co-Hydrothermal Carbonization of Agricultural Waste and Sewage Sludge for Product Quality Improvement: Fuel Properties of Hydrochar and Fertilizer Quality of Aqueous Phase. *J Environ Manage* **2023**, *326*, 116781, doi:10.1016/j.jenvman.2022.116781.
11. Li, H.Z.; Zhang, Y.N.; Guo, J.Z.; Lv, J.Q.; Huan, W.W.; Li, B. Preparation of Hydrochar with High Adsorption Performance for Methylene Blue by Co-Hydrothermal Carbonization of Polyvinyl Chloride and Bamboo. *Bioresour Technol* **2021**, *337*, doi:10.1016/j.biortech.2021.125442.
12. Cavali, M.; Benbelkacem, H.; Kim, B.; Bayard, R.; Libardi Junior, N.; Gonzaga Domingos, D.; Woiciechowski, A.L.; Castilhos Junior, A.B. de Co-Hydrothermal Carbonization of Pine Residual Sawdust and Non-Dewatered Sewage Sludge – Effect of Reaction Conditions on Hydrochar Characteristics. *J Environ Manage* **2023**, *340*, 117994, doi:10.1016/J.JENVMAN.2023.117994.
13. Masoumi, S.; Borugadda, V.B.; Nanda, S.; Dalai, A.K. Hydrochar: A Review on Its Production Technologies and Applications. *Catalysts* 2021, *11*.
14. Katheresan, V.; Kansedo, J.; Lau, S.Y. Efficiency of Various Recent Wastewater Dye Removal Methods: A Review. *J Environ Chem Eng* 2018, *6*, 4676–4697.
15. Dutta, S.; Adhikary, S.; Bhattacharya, S.; Roy, D.; Chatterjee, S.; Chakraborty, A.; Banerjee, D.; Ganguly, A.; Nanda, S.; Rajak, P. Contamination of Textile Dyes in Aquatic Environment: Adverse Impacts on Aquatic Ecosystem and Human Health, and Its Management Using Bioremediation. *J Environ Manage* 2024, *353*.

16. Al-Tohamy, R.; Ali, S.S.; Li, F.; Okasha, K.M.; Mahmoud, Y.A.G.; Elsamahy, T.; Jiao, H.; Fu, Y.; Sun, J. A Critical Review on the Treatment of Dye-Containing Wastewater: Ecotoxicological and Health Concerns of Textile Dyes and Possible Remediation Approaches for Environmental Safety. *Ecotoxicol Environ Saf* 2022, *231*.
17. Merzari, F.; Langone, M.; Andreottola, G.; Fiori, L. *Methane Production from Process Water of Sewage Sludge Hydrothermal Carbonization. A Review. Valorising Sludge through Hydrothermal Carbonization*; 2019; Vol. 49; ISBN 2013187955.
18. Wirth, B.; Reza, T.; Mumme, J. Influence of Digestion Temperature and Organic Loading Rate on the Continuous Anaerobic Treatment of Process Liquor from Hydrothermal Carbonization of Sewage Sludge. *Bioresour Technol* **2015**, *198*, 215–222, doi:10.1016/j.biortech.2015.09.022.
19. Liu, T.; Tian, L.; Liu, Z.; He, J.; Fu, H.; Huang, Q.; Xue, H.; Huang, Z. Distribution and Toxicity of Polycyclic Aromatic Hydrocarbons during CaO-Assisted Hydrothermal Carbonization of Sewage Sludge. *Waste Management* **2021**, *120*, 616–625, doi:10.1016/j.wasman.2020.10.025.
20. Fregolente, L.G.; Miguel, T.B.A.R.; de Castro Miguel, E.; de Almeida Melo, C.; Moreira, A.B.; Ferreira, O.P.; Bisinoti, M.C. Toxicity Evaluation of Process Water from Hydrothermal Carbonization of Sugarcane Industry By-Products. *Environmental Science and Pollution Research* **2019**, *26*, 27579–27589, doi:10.1007/s11356-018-1771-2.
21. Petrovič, A.; Cenčič Predikaka, T.; Škodič, L.; Vohl, S.; Čuček, L. Hydrothermal Co-Carbonization of Sewage Sludge and Whey: Enhancement of Product Properties and Potential Application in Agriculture. *Fuel* **2023**, *350*, doi:10.1016/j.fuel.2023.128807.
22. Kusuma, H.S.; Christa Jaya, D.E.; Illiyanasafa, N.; Ikawati, K.L.; Kurniasari, E.; Darmokoesoemo, H.; Amenaghawon, A.N. A Critical Review and Bibliometric Analysis of Methylene Blue Adsorption Using Leaves. *Chemosphere* **2024**, *356*, doi:10.1016/j.chemosphere.2024.141867.
23. Khan, I.; Saeed, K.; Zekker, I.; Zhang, B.; Hendi, A.H.; Ahmad, A.; Ahmad, S.; Zada, N.; Ahmad, H.; Shah, L.A.; et al. Review on Methylene Blue: Its Properties, Uses, Toxicity and Photodegradation. *Water (Switzerland)* 2022, *14*.
24. Oladoye, P.O.; Ajiboye, T.O.; Omotola, E.O.; Oyewola, O.J. Methylene Blue Dye: Toxicity and Potential Elimination Technology from Wastewater. *Results in Engineering* 2022, *16*.
25. Cavali, M.; Kim, B.; Tedoldi, D.; Benbelkacem, H.; Bayard, R.; Garnier, V.; Libardi, N.; Woiciechowski, A.L.; Borges de Castilhos, A. Hydrochar from Sawdust and Sewage Sludge–a Potential Media for Retaining Heavy Metals in Sustainable Drainage Systems (SuDS). *Environmental Technology (United Kingdom)* **2024**, doi:10.1080/09593330.2024.2411066.
26. Velinov, N.; Najdanović, S.; Vučić, R.; Mitrović, J.; Kostić, M.; Bojić, D.; Bojić, A. *BIOSORPTION OF LOPERAMIDE BY LIGNOCELLULOSIC-Al 2 O 3 HYBRID: OPTIMIZATION, KINETICS, ISOTHERMAL AND THERMODYNAMIC STUDIES*; 2019; Vol. 53;.
27. Filipović, K.; Petrović, M.; Najdanović, S.; Velinov, N.; Hurt, A.; Bojić, A.; Kostić, M. Highly Efficient Nano Sorbent as a Superior Material for the Purification of Wastewater Contaminated with Anthraquinone Dye RB19. *Journal of Water Process Engineering* **2024**, *67*, doi:10.1016/j.jwpe.2024.106118.
28. Isquierdo, E.P.; Caldeira, D.S.A.; Siqueira, V.C.; Martins, E.A.S.; Quequeto, W.D. Fittings of Adsorption Isotherm Models and Thermodynamic Properties of Urunday Seeds. *Engenharia Agricola* **2020**, *40*, 374–380, doi:10.1590/1809-4430-ENG.AGRIC.V40N3P374-380/2020.
29. Velinov, N.; Radović Vučić, M.; Petrović, M.; Najdanović, S.; Kostić, M.; Mitrović, J.; Bojić, A. The Influence of Various Solvents' Polarity in the Synthesis of Wood Biowaste Sorbent: Evaluation of Dye Sorption. *Biomass Convers Biorefin* **2023**, *13*, 8139–8150, doi:10.1007/s13399-021-01691-8.
30. Chambers, C.; Saha, S.; Grimes, S.; Calhoun, J.; Reza, M.T. Physical and Morphological Alteration of Sargassum-Derived Ultraporous Superactivated Hydrochar with Remarkable Cationic Dye Adsorption. *Biomass Convers Biorefin* **2023**, doi:10.1007/s13399-023-04326-2.

31. Aktas, K.; Liu, H.; Eskicioglu, C. Treatment of Aqueous Phase from Hydrothermal Liquefaction of Municipal Sludge by Adsorption: Comparison of Biochar, Hydrochar, and Granular Activated Carbon. *J Environ Manage* **2024**, *356*, doi:10.1016/j.jenvman.2024.120619.
32. Alhawtali, S.; El-Harbawi, M.; Al-Awadi, A.S.; El Blidi, L.; Alrashed, M.M.; Yin, C.Y. Enhanced Adsorption of Methylene Blue Using Phosphoric Acid-Activated Hydrothermal Carbon Microspheres Synthesized from a Variety of Palm-Based Biowastes. *Coatings* **2023**, *13*, doi:10.3390/coatings13071287.
33. Genli, N.; Kutluay, S.; Baytar, O.; Şahin, Ö. Preparation and Characterization of Activated Carbon from Hydrochar by Hydrothermal Carbonization of Chickpea Stem: An Application in Methylene Blue Removal by RSM Optimization. *Int J Phytoremediation* **2022**, *24*, 88–100, doi:10.1080/15226514.2021.1926911.
34. Md. Munjur, H.; Hasan, M.N.; Awual, M.R.; Islam, M.M.; Shenashen, M.A.; Iqbal, J. Biodegradable Natural Carbohydrate Polymeric Sustainable Adsorbents for Efficient Toxic Dye Removal from Wastewater. *J Mol Liq* **2020**, *319*, doi:10.1016/j.molliq.2020.114356.
35. American Public Health Association, A. *Standard Methods for the Examination of Water and Wastewater*; Baird, R.B., Eaton, A.D., Rice, E.W., Eds.; 23rd ed.; Washington, DC, 2017; ISBN 9780875532875.
36. Atallah, E.; Kwapinski, W.; Ahmad, M.N.; Leahy, J.J.; Al-Muhtaseb, A.H.; Zeaiter, J. Hydrothermal Carbonization of Olive Mill Wastewater: Liquid Phase Product Analysis. *J Environ Chem Eng* **2019**, *7*, doi:10.1016/j.jece.2018.102833.
37. Zhou, F.; Li, K.; Hang, F.; Zhang, Z.; Chen, P.; Wei, L.; Xie, C. Efficient Removal of Methylene Blue by Activated Hydrochar Prepared by Hydrothermal Carbonization and NaOH Activation of Sugarcane Bagasse and Phosphoric Acid. *RSC Adv* **2022**, *12*, 1885–1896, doi:10.1039/d1ra08325b.
38. Khoshbouy, R.; Takahashi, F.; Yoshikawa, K. Preparation of High Surface Area Sludge-Based Activated Hydrochar via Hydrothermal Carbonization and Application in the Removal of Basic Dye. *Environ Res* **2019**, *175*, 457–467, doi:10.1016/j.envres.2019.04.002.
39. Dhaouadi, F.; Sellaoui, L.; Hernández-Hernández, L.E.; Bonilla-Petriciolet, A.; Mendoza-Castillo, D.I.; Reynel-Ávila, H.E.; González-Ponce, H.A.; Taamalli, S.; Louis, F.; Lamine, A. Ben Preparation of an Avocado Seed Hydrochar and Its Application as Heavy Metal Adsorbent: Properties and Advanced Statistical Physics Modeling. *Chemical Engineering Journal* **2021**, *419*, 129472, doi:10.1016/J.CEJ.2021.129472.
40. Zhou, N.; Chen, H.; Feng, Q.; Yao, D.; Chen, H.; Wang, H.; Zhou, Z.; Li, H.; Tian, Y.; Lu, X. Effect of Phosphoric Acid on the Surface Properties and Pb(II) Adsorption Mechanisms of Hydrochars Prepared from Fresh Banana Peels. *J Clean Prod* **2017**, *165*, 221–230, doi:10.1016/J.JCLEPRO.2017.07.111.
41. Xue, Y.; Gao, B.; Yao, Y.; Inyang, M.; Zhang, M.; Zimmerman, A.R.; Ro, K.S. Hydrogen Peroxide Modification Enhances the Ability of Biochar (Hydrochar) Produced from Hydrothermal Carbonization of Peanut Hull to Remove Aqueous Heavy Metals: Batch and Column Tests. *Chemical Engineering Journal* **2012**, *200–202*, 673–680, doi:10.1016/J.CEJ.2012.06.116.
42. Saha, N.; Volpe, M.; Fiori, L.; Volpe, R.; Messineo, A.; Reza, M.T. Cationic Dye Adsorption on Hydrochars of Winery and Citrus Juice Industries Residues: Performance, Mechanism, and Thermodynamics. *Energies (Basel)* **2020**, *13*, doi:10.3390/en13184686.
43. Ferrentino, R.; Ceccato, R.; Marchetti, V.; Andreottola, G.; Fiori, L. Sewage Sludge Hydrochar: An Option for Removal of Methylene Blue from Wastewater. *Applied Sciences (Switzerland)* **2020**, *10*, doi:10.3390/app10103445.
44. El Ouadrhiri, F.; Elyemni, M.; Lahkimi, A.; Lhassani, A.; Chaouch, M.; Taleb, M. Mesoporous Carbon from Optimized Date Stone Hydrochar by Catalytic Hydrothermal Carbonization Using Response Surface Methodology: Application to Dyes Adsorption. *International Journal of Chemical Engineering* **2021**, *2021*, doi:10.1155/2021/5555406.
45. El Ouadrhiri, F.; Abdu Musad Saleh, E.; Husain, K.; Adachi, A.; Hmamou, A.; Hassan, I.; Mostafa Moharam, M.; Lahkimi, A. Acid Assisted-Hydrothermal Carbonization of Solid Waste from Essential Oils Industry: Optimization Using I-Optimal Experimental Design and Removal Dye Application. *Arabian Journal of Chemistry* **2023**, *16*, doi:10.1016/j.arabjc.2023.104872.

46. Zhou, S.; Hu, A.; Jiang, J.; Tang, J.; Zhou, G.; Zhu, L.; Wang, S. Low-Temperature Synthesized Hierarchical Porous Carbon from Waste Hydrochar with Super Capacity for Dye Adsorption. *Biomass Bioenergy* **2023**, *177*, doi:10.1016/j.biombioe.2023.106938.
47. Lin, Z.; Wang, R.; Tan, S.; Zhang, K.; Yin, Q.; Zhao, Z.; Gao, P. Nitrogen-Doped Hydrochar Prepared by Biomass and Nitrogen-Containing Wastewater for Dye Adsorption: Effect of Nitrogen Source in Wastewater on the Adsorption Performance of Hydrochar. *J Environ Manage* **2023**, *334*, doi:10.1016/j.jenvman.2023.117503.
48. Hessien, M. Methylene Blue Dye Adsorption on Iron Oxide-Hydrochar Composite Synthesized via a Facile Microwave-Assisted Hydrothermal Carbonization of Pomegranate Peels' Waste. *Molecules* **2023**, *28*, doi:10.3390/molecules28114526.
49. Santoso, E.; Ediati, R.; Kusumawati, Y.; Bahruji, H.; Sulistiono, D.O.; Prasetyoko, D. Review on Recent Advances of Carbon Based Adsorbent for Methylene Blue Removal from Waste Water. *Mater Today Chem* 2020, *16*.
50. Mozaffari Majd, M.; Kordzadeh-Kermani, V.; Ghalandari, V.; Askari, A.; Sillanpää, M. Adsorption Isotherm Models: A Comprehensive and Systematic Review (2010–2020). *Science of the Total Environment* 2022, *812*.
51. de Vargas Brião, G.; Hashim, M.A.; Chu, K.H. The Sips Isotherm Equation: Often Used and Sometimes Misused. *Separation Science and Technology (Philadelphia)* 2023, *58*, 884–892.
52. Liu, J.L.; Qian, W.C.; Guo, J.Z.; Shen, Y.; Li, B. Selective Removal of Anionic and Cationic Dyes by Magnetic Fe3O4-Loaded Amine-Modified Hydrochar. *Bioresour Technol* **2021**, *320*, doi:10.1016/j.biortech.2020.124374.
53. Akbari, A.; Peighambardoust, S.J.; Lotfi, M. Hydrochar Derived from Liquorice Root Pulp Utilizing Catalytic/Non-Catalytic Hydrothermal Carbonization: RSM Optimization and Cationic Dye Adsorption Assessment. *Journal of Water Process Engineering* **2023**, *55*, doi:10.1016/j.jwpe.2023.104099.
54. Kajjumba, G.W.; Emik, S.; Öngen, A.; Kurtulus Özcan, H.; Aydın, S. Modelling of Adsorption Kinetic Processes-Errors, Theory and Application. In *Advanced Sorption Process Applications*; Edebali, S., Ed.; IntechOpen, 2019.
55. Wang, J.; Guo, X. Adsorption Kinetic Models: Physical Meanings, Applications, and Solving Methods. *J Hazard Mater* 2020, *390*.
56. Wu, F.C.; Tseng, R.L.; Juang, R.S. Characteristics of Elovich Equation Used for the Analysis of Adsorption Kinetics in Dye-Chitosan Systems. *Chemical Engineering Journal* **2009**, *150*, 366–373, doi:10.1016/j.cej.2009.01.014.
57. Parmar, K.R.; Ross, A.B. Integration of Hydrothermal Carbonisation with Anaerobic Digestion - Opportunities for Valorisation of Digestate. *Energies (Basel)* **2019**, *12*, doi:10.3390/en12091586.
58. Murillo, H.A.; Pagés-Díaz, J.; Díaz-Robles, L.A.; Vallejo, F.; Huiliñir, C. Valorization of Oat Husk by Hydrothermal Carbonization: Optimization of Process Parameters and Anaerobic Digestion of Spent Liquors. *Bioresour Technol* **2022**, *343*, doi:10.1016/j.biortech.2021.126112.
59. Brown, A.E.; Adams, J.M.M.; Grasham, O.R.; Camargo-Valero, M.A.; Ross, A.B. An Assessment of Different Integration Strategies of Hydrothermal Carbonisation and Anaerobic Digestion of Water Hyacinth. *Energies (Basel)* **2020**, *13*, doi:10.3390/en13225983.
60. Farru, G.; Cappai, G.; Carucci, A.; De Gioannis, G.; Asunis, F.; Milia, S.; Muntoni, A.; Perra, M.; Serpe, A. A Cascade Biorefinery for Grape Marc: Recovery of Materials and Energy through Thermochemical and Biochemical Processes. *Science of the Total Environment* **2022**, *846*, doi:10.1016/j.scitotenv.2022.157464.
61. Aragón-Briceño, C.; Ross, A.B.; Camargo-Valero, M.A. Evaluation and Comparison of Product Yields and Bio-Methane Potential in Sewage Digestate Following Hydrothermal Treatment. *Appl Energy* **2017**, *208*, 1357–1369, doi:10.1016/j.apenergy.2017.09.019.
62. Bamba, D.; Coulibaly, M.; Robert, D. Nitrogen-Containing Organic Compounds: Origins, Toxicity and Conditions of Their Photocatalytic Mineralization over TiO2. *Science of the Total Environment* 2017, *580*, 1489–1504.
63. Farru, G.; Dang, C.H.; Schultze, M.; Kern, J.; Cappai, G.; Libra, J.A. Benefits and Limitations of Using Hydrochars from Organic Residues as Replacement for Peat on Growing Media. *Horticulturae* **2022**, *8*, doi:10.3390/horticulturae8040325.

64. Petrovič, A.; Cenčič Predikaka, T.; Parlov Vuković, J.; Jednačak, T.; Hribernik, S.; Vohl, S.; Urbancl, D.; Tišma, M.; Čuček, L. Sustainable Hydrothermal Co-Carbonization of Residues from the Vegetable Oil Industry and Sewage Sludge: Hydrochar Production and Liquid Fraction Valorisation. *Energy* **2024**, *307*, doi:10.1016/j.energy.2024.132760.
65. Mantovani, M.; Collina, E.; Marazzi, F.; Lasagni, M.; Mezzanotte, V. Microalgal Treatment of the Effluent from the Hydrothermal Carbonization of Microalgal Biomass. *Journal of Water Process Engineering* **2022**, *49*, doi:10.1016/j.jwpe.2022.102976.
66. Czerwińska, K.; Marszałek, A.; Kudlek, E.; Śliz, M.; Dudziak, M.; Wilk, M. The Treatment of Post-Processing Liquid from the Hydrothermal Carbonization of Sewage Sludge. *Science of the Total Environment* **2023**, *885*, doi:10.1016/j.scitotenv.2023.163858.
67. Cavali, M.; Ricardo Soccol, C.; Tavares, D.; Alberto Zevallos Torres, L.; Oliveira de Andrade Tanobe, V.; Zandoná Filho, A.; Lorenci Woiciechowski, A. Effect of Sequential Acid-Alkaline Treatment on Physical and Chemical Characteristics of Lignin and Cellulose from Pine (Pinus Spp.) Residual Sawdust. *Bioresour Technol* **2020**, 123884, doi:10.1016/j.biortech.2020.123884.
68. Cavali, M.; Soccol, C.R.; Tavares, D.; Zevallos Torres, L.A.; Oliveira de Andrade Tanobe, V.; Zandoná Filho, A.; Woiciechowski, A.L. Valorization of Lignin from Pine (Pinus Spp.) Residual Sawdust: Antioxidant Activity and Application in the Green Synthesis of Silver Nanoparticles for Antibacterial Purpose. *Biomass Convers Biorefin* **2021**, doi:10.1007/s13399-021-01940-w.
69. Zhu, J.Y.; Pan, X. Efficient Sugar Production from Plant Biomass: Current Status, Challenges, and Future Directions. *Renewable and Sustainable Energy Reviews* 2022, *164*.
70. Wang, Y.; Zhang, Y.; Cui, Q.; Feng, Y.; Xuan, J. Composition of Lignocellulose Hydrolysate in Different Biorefinery Strategies: Nutrients and Inhibitors. *Molecules* 2024, *29*.
71. Ischia, G.; Fiori, L. Hydrothermal Carbonization of Organic Waste and Biomass: A Review on Process, Reactor, and Plant Modeling. *Waste Biomass Valorization* 2021, *12*, 2797–2824.
72. Petrovič, A.; Cenčič Predikaka, T.; Škodič, L.; Vohl, S.; Čuček, L. Hydrothermal Co-Carbonization of Sewage Sludge and Whey: Enhancement of Product Properties and Potential Application in Agriculture. *Fuel* **2023**, *350*, doi:10.1016/j.fuel.2023.128807.
73. Bozell, J.J.; Petersen, G.R. Technology Development for the Production of Biobased Products from Biorefinery Carbohydrates—the US Department of Energy's "Top 10" Revisited. *Green Chemistry* **2010**, *12*, 539–555, doi:10.1039/b922014c.
74. Faure, E.; Falentin-Daudré, C.; Jérôme, C.; Lyskawa, J.; Fournier, D.; Woisel, P.; Detrembleur, C. Catechols as Versatile Platforms in Polymer Chemistry. *Prog Polym Sci* 2013, *38*, 236–270.
75. Mariscal, R.; Maireles-Torres, P.; Ojeda, M.; Sádaba, I.; López Granados, M. Furfural: A Renewable and Versatile Platform Molecule for the Synthesis of Chemicals and Fuels. *Energy Environ Sci* 2016, *9*, 1144–1189.
76. Fache, M.; Darroman, E.; Besse, V.; Auvergne, R.; Caillol, S.; Boutevin, B. Vanillin, a Promising Biobased Building-Block for Monomer Synthesis. *Green Chemistry* **2014**, *16*, 1987–1998, doi:10.1039/c3gc42613k.